Journal of Photochemistry, 13 (1980) 149 - 163

PHOTOLYSIS OF METHYL NITRITE: KINETICS OF THE REACTION OF THE METHOXY RADICAL WITH O_2

R. A. COX, R. G. DERWENT and S. V. KEARSEY*
Environmental and Medical Sciences Division, A.E.R.E., Harwell, Oxfordshire (Gt. Britain)
L. BATT and K. G. PATRICK
Department of Chemistry, University of Aberdeen, Old Aberdeen (Gt. Britain)
(Received November 29, 1979)

Summary

The near-UV photolysis of methyl nitrite in the presence of oxygen was investigated at pressures near 1 atm. The initial process is

$$CH_3ONO + h\nu \rightarrow CH_3O + NO$$

which occurs with a quantum yield of unity under the conditions used in this work. The primary products react further by a complex mechanism to yield a variety of products which include NO_2, HNO_3, HCHO and CH_3ONO_2. Methyl nitrate exhibits a strong dependence on O_2 and NO_2; this could be interpreted in terms of competition between the reactions

$$CH_3O + NO_2\ (+M) \rightarrow CH_3ONO_2\ (+M) \quad (5)$$

$$CH_3O + O_2 \rightarrow HCHO + HO_2 \quad (4)$$

The ratio k_4/k_5 was determined by computer simulation of the experimental data over a range of temperatures and compositions and k_4 was evaluated using a literature value for k_5. By combining all the available data for k_4 over the temperature range 296 - 450 K the following Arrhenius expression was derived:

$$k_4 = (1.26^{+1.90}_{-0.76}) \times 10^{-13} \exp\{-(1352 \pm 340)/T\}\ \text{cm}^3\ \text{molecule}^{-1}\ \text{s}^{-1}$$

1. Introduction

It is now reasonably well established that the primary process in the photolysis of alkyl nitrites of low molecular weight in their near-UV absorption band is dissociation to give alkoxy radicals [1]. Thus photolysis of methyl nitrite provides a convenient source of methoxy radicals:

*Present address: Science Department, University of Durham, South Road, Durham, Gt. Britain.

$$CH_3ONO + h\nu \rightarrow CH_3O + NO \quad (1)$$

The chemical behaviour of CH_3O in systems containing O_2 (or air) and the nitrogen oxides NO and NO_2 is of particular interest in connection with atmospheric chemistry, where CH_3O is believed to be an intermediate in the oxidation of methyl radicals to formaldehyde by the reactions [2]

$$CH_3 + O_2 + M \rightarrow CH_3O_2 + M \quad (2)$$

$$CH_3O_2 + NO \rightarrow CH_3O + NO_2 \quad (3)$$

$$CH_3O + O_2 \rightarrow HCHO + HO_2 \quad (4)$$

Very strong evidence for the production of CH_3O and the occurrence of reaction (4) comes from a flash photolysis study of CH_3ONO [3], where rapid production of OH has been observed to follow the flash. This can readily be explained by reaction (4) followed by the fast reaction of HO_2 with the NO produced in reaction (1). Unfortunately there have been no direct measurements to date of the rate constants for reaction (4) or any other reactions of the CH_3O radical. However, there is much information, sometimes apparently conflicting, on the relative rates of CH_3O reactions, obtained from product analysis studies of chemical systems of greater or lesser complexity.

Two recent studies have yielded measurements of k_4 relative to the reaction of CH_3O with NO_2 (k_5) using dimethyl peroxide as a thermal source of CH_3O.

$$CH_3O + NO_2 (+M) \rightarrow CH_3ONO_2 (+M) \quad (5)$$

Barker *et al.* [4] have monitored changes in the total pressure and in $[NO_2]$ and Batt and Robinson [5] have used gas chromatographic analysis to determine the amount of CH_3ONO_2 formed from dimethyl peroxide–O_2–NO_2 mixtures. Both groups have been able to deduce values of k_4/k_5 from their data over a limited temperature range around 400 K; the results are in moderately good agreement.

The photolysis of methyl nitrite in the presence of O_2 has been used previously to obtain a value for k_4 relative to the reaction of CH_3O with NO [6].

$$CH_3O + NO (+M) \rightarrow CH_3ONO (+M) \quad (6)$$

The relative rates obtained in this study at room temperature seem to be consistent with a recent study of the photo-oxidation of CH_4 in the presence of NO and NO_2 carried out in our laboratory [2]. Methyl nitrite photolysis in O_2 and air has also been studied by Gay *et al.* [7] who have identified the major products by Fourier transform IR spectroscopy. The data are entirely consistent with reaction (1) being the major photochemical pathway.

The importance of reaction (4) has also been recognized in low temperature combustion systems where CH_3O is generated as a secondary radical during the oxidation of CH_3. Some of these data at room temperature [8, 9]

point to a much lower value for k_4 than is indicated from the aforementioned studies. However, the higher temperature data [10 - 12] are reasonably compatible with the recent dimethyl peroxide decomposition studies [4, 5].

The present study was initiated in order to confirm the mechanism of photo-oxidation of methyl nitrite at room temperature and to use this system to obtain a value for k_4, in a temperature range intermediate between that employed in the previous photochemical and thermal studies, relative to the association reaction (5).

2. Experimental

Two experimental systems were used in this study of the photolysis of methyl nitrite. Most of the data at room temperature (298 ± 3 K) were obtained using low concentrations of CH_3ONO ($(1 - 5) \times 10^{14}$ molecules cm^{-3}) diluted in O_2 or $O_2 + N_2$ mixtures at atmospheric pressure and contained in a 250 l bag made of polyvinylfluoride film (Dupont "Tedlar"). The bag was positioned between two banks of 20 W fluorescent blacklights (Philips TL 20/08) which gave homogeneous radiation in the region 310 - 410 nm, with maximum intensity at 350 nm.

The concentrations of CH_3ONO and its photolysis products were followed as a function of time by withdrawing successive samples, using a small pump, through a polytetrafluoroethylene tube which projected into the centre of the bag. Gases entered the bag through a similar tube and CH_3ONO and other reactants were introduced as aliquots of the pure compound, which were flushed into the bag in a stream of diluent (N_2 or O_2). Analysis of CH_3ONO and CH_3ONO_2 was by gas chromatography using flame ionization detection (FID) and electron capture (EC) detection respectively. Separation was achieved on a 2 m glass column containing PEG400 on Chromosorb and the system was calibrated using pure samples of the compounds diluted in N_2 and O_2. A commercial chemiluminescence analyser (TECO Model 12A) was used to analyse for NO and NO_x. In the NO_x mode the instrument responded quantitatively to NO, NO_2, HONO, CH_3ONO and CH_3ONO_2 but did not respond to HNO_3. HONO, which was not normally present in detectable amounts, could be distinguished by its high solubility in aqueous alkali [2]. The NO_2 was determined by subtraction of the measured concentrations of NO, CH_3ONO and CH_3ONO_2 from the total NO_x signal. The decline in total NO_x during photolysis was assumed to be a measure of the HNO_3 formed. In a few experiments ozone was measured by chemiluminescence from the $O_3 + C_2H_4$ reaction. Analysis for formaldehyde was carried out using the MBTH colorimetric method as described previously [2]. Possible interference from other photolysis products could not be checked easily and the overall accuracy of the data for HCHO is uncertain.

The study of methyl nitrite photolysis at higher temperatures was carried out using a more conventional photolysis system comprising a cylindrical quartz cell, 15 cm long and 3.8 cm in diameter, mounted in a steel

block furnace and attached to a vacuum system. A parallel beam of 366 nm light, isolated using filters from a medium pressure mercury arc (Osram/Thorn Type ME), passed axially through the cell and was monitored on a blue-sensitive photocell. The light intensity showed little change with time and excellent reproducibility from day to day. Mixtures of CH_3ONO (6×10^{16} molecules cm^{-3}) with other reactants were prepared in the photolysis cell, allowed to mix for 2 h and irradiated for 5 min. The contents of the cell were then quenched in liquid N_2 and the non-condensable gases were pumped off prior to gas chromatographic analysis. CH_3ONO and CH_3ONO_2 were separated on a 2 m column containing 20% β,β'-oxydipropionitrile on Chromosorb and detected by FID. In runs with added isobutane, the residual i-C_4H_{10} was removed by pumping at 173 K and methyl ethyl ketone was added as an internal standard to monitor losses of CH_3ONO during this operation.

Methyl nitrite was prepared either by reaction of CH_3OH with acidified $NaNO_2$ or by exchange between methanol and commercial amyl nitrite (BDH). The product, which was purified by fractional distillation, was stored in the dark. The only detectable impurity was 0.3% CH_3OH. Methyl nitrate was prepared by the reaction of methanol with a concentrated H_2SO_4–HNO_3 mixture at 273 K in the presence of urea. The dried product contained no impurities detectable by gas–liquid chromatography. N_2 (high purity) and O_2 (breathing grade) were used as supplied by BOC.

3. Results and discussion

3.1. The photolysis of low concentrations of CH_3ONO in N_2 + O_2

Figure 1 shows the concentration–time behaviour of the reactant and several products in the photolysis of 9.47 ppm CH_3ONO in 1 atm of N_2 + 25% O_2 at room temperature (1 ppm $\approx 2.45 \times 10^{13}$ molecules cm^{-3} at 760 Torr and 298 K). The main products formed initially are NO, NO_2 and HCHO but all of these are consumed in secondary reactions. NO declines very quickly after an initial sharp rise, whereas concentration maxima for HCHO and NO_2 are attained after about 30 min. The rates of formation of methyl nitrate and nitric acid increase with time, indicating that these are secondary products. These observations are entirely consistent with those of Gay *et al.* [7], who also observed O_3, N_2O_5, CO and HCOOH as secondary products; consideration of the carbon balance has shown that the CO and HCOOH can be entirely accounted for by oxidation of HCHO.

The kinetic behaviour illustrated in Fig. 1 was typical of that observed over a variety of conditions. The initial methyl nitrite concentration was varied from 2 to 20 ppm and in some cases NO_2 (up to 4.4 ppm) was added. The fraction of O_2 in the diluent gas was varied between 3.5 and 100%. These changes in composition did not noticeably affect the first order decay rate of CH_3ONO (see Section 3.2) but the yield of methyl nitrate was sensitive to the relative amounts of O_2 and NO_2 present.

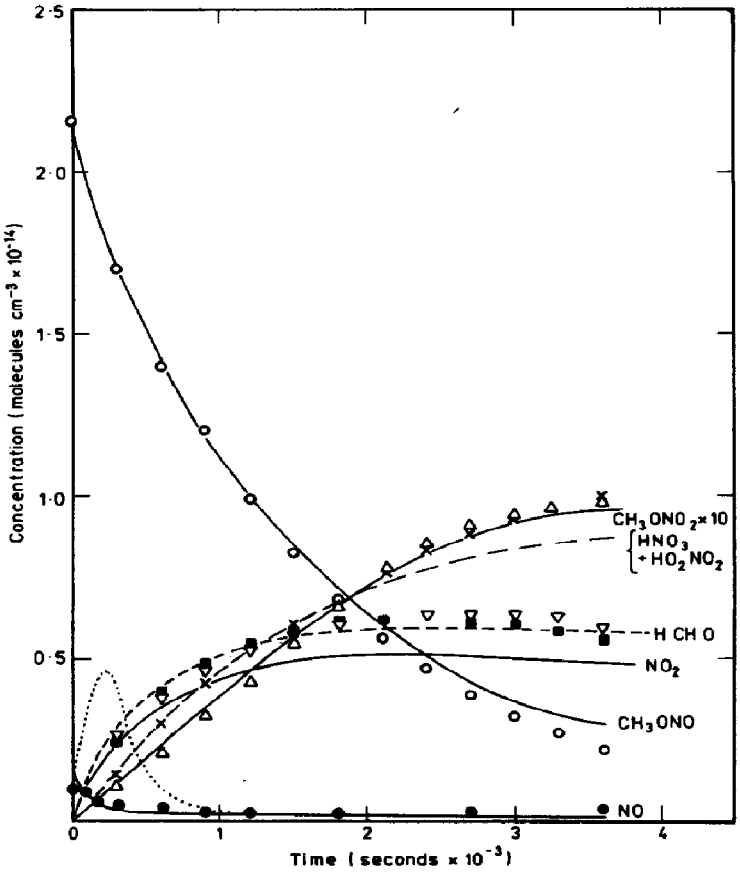

Fig. 1. Concentration–time behaviour in the photolysis of CH_3ONO in the presence of N_2 + 25% O_2 at atmospheric pressure and room temperature. Experimental points: ○, CH_3ONO; ●, NO (× 10); ▽, NO_2; △, CH_3ONO_2; ×, "HNO_3"; ■, HCHO. Computed curves: (see text) as labelled; ..., computed curve for NO without addition routes for the OH + CH_3ONO reaction.

3.2. Kinetics of the decay of CH_3ONO and the quantum yield for photodissociation

The decay of methyl nitrite as a function of time is shown in Fig. 2. CH_3ONO removal is approximately first order to at least 90% decomposition and the rate is proportional to the number of fluorescent lamps activated. This indicates that primary photodissociation is the dominant loss process for CH_3ONO and that secondary reactions are relatively unimportant. This was confirmed in computer simulations which are described in Section 3.4. These simulations show that the decay rate constant for CH_3ONO, as determined from logarithmic plots such as those given in Fig. 2, is 20% greater than the photolysis rate constant k_1. The quantum yield $\Phi(CH_3ONO)$ for CH_3ONO photolysis was estimated by comparing the photolysis rate constants for CH_3ONO, HONO and NO_2 with the estimated relative rates of light absorption of these species in the reactor. The latter were calculated from

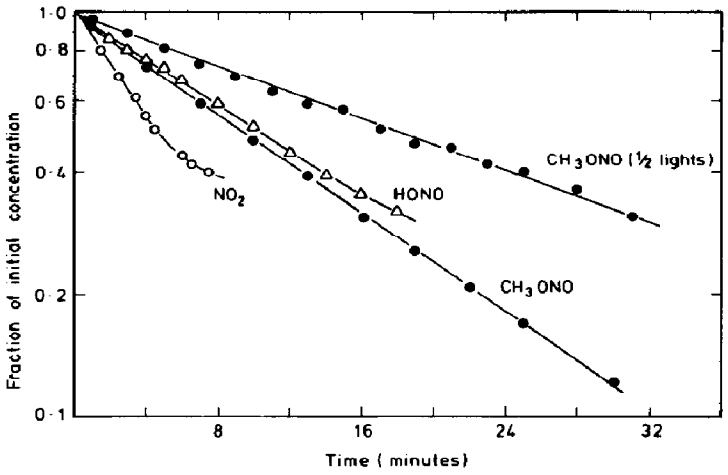

Fig. 2. Decay curves for the photolysis of NO_2, HONO and CH_3ONO in the presence of N_2 or N_2 + O_2 at a pressure of 1 atm.

the overlap of the absorption cross sections σ_λ for CH_3ONO [1], HONO [13] and NO_2 [14] and the intensity function of the light source was measured using a photometer. The individual products $I_\lambda\sigma_\lambda$ were averaged over 5 nm and the absorption rate was calculated from $k_a = \sum_\lambda I_\lambda\sigma_\lambda$ in arbitrary units, with an estimated error of ±5%.

Figure 2 also shows decay plots for HONO, measured during the photolysis of a mixture containing initially HONO (9.2 ppm), NO_2 (1.6 ppm) and NO (1.2 ppm) diluted in 1 atm of N_2 + 40% O_2, and for NO_2, measured during the photolysis of a mixture of NO_2 (8.5 ppm) and NO (2.5 ppm) in N_2. Both decay plots are curved since the HONO and NO_2 photolyses proceed by complex mechanisms. In order to extract the primary dissociation rate from the observed decay curves shown in Fig. 2, the data were analysed using previously described methods and kinetic information from this laboratory for HONO photolysis [15] and from the work of Wu and Niki [16] for NO_2 photolysis. The results are summarized in Table 1 which shows the photodissociation rates, the light absorption rates and the values of $\Phi(CH_3ONO)$ calculated on the basis of the established unit quantum yields for the photodissociation of HONO and NO_2 [17, 18], *i.e.*

$$\Phi(CH_3ONO) = \frac{k_1}{k_{27}}\frac{k_a^{HONO}}{k_a^{CH_3ONO}} = \frac{k_1}{k_{21}}\frac{k_a^{NO_2}}{k_a^{CH_3ONO}}$$

where k_{27} and k_{21} are the rate constants for the processes

$$HONO + h\nu \longrightarrow HO + NO \qquad (27)$$

$$NO_2 + h\nu \longrightarrow NO + O \qquad (21)$$

Considering the experimental error in this determination (±10%), a comparison with the HONO photolysis data suggests that $\Phi(CH_3ONO) = 1$ but the NO_2 photolysis data give a slightly larger value. The higher value is probably

TABLE 1

Quantum yields for photodissociation of CH_3ONO

Photochemical reactant	*Light absorption rate (relative)*	*Photodissociation rate* ($s^{-1} \times 10^4$)	$\Phi(CH_3ONO)$
CH_3ONO	1.0	9.7 ± 1.2	–
HONO	0.71	7.2 ± 0.8	0.96
NO_2	2.5	20.5 ± 0.22	1.18

caused by underestimation of k_{21} due to impurity O_2 in the photolysis mixtures. Significant errors can be introduced into the determination of k_2 if the O_2 level is more than 100 times greater than the NO_2 level, *i.e.* approximately 10^3 ppm, and impurity O_2 levels of this order are very likely to be present in the bag mixtures prepared in this study. It is concluded therefore that the primary photodissociation of CH_3ONO proceeds with a quantum yield of unity.

3.3. The photolysis of higher concentrations of methyl nitrite: temperature dependence of methyl nitrate formation

To confirm the nature of the initial photodissociation of CH_3ONO and to measure its rate, the photolysis of CH_3ONO (6×10^{16} molecules cm^{-3}) was studied in the presence of isobutane (approximately 1.5×10^{20} molecules cm^{-3}) at 100 °C. The only products detected were methanol and 2-methyl-2-nitrosopropane, showing that the following reactions dominate the chemistry:

$$CH_3ONO + h\nu \longrightarrow CH_3O + NO$$

$$CH_3O + i\text{-}C_4H_{10} \longrightarrow CH_3OH + t\text{-}C_4H_9$$

$$t\text{-}C_4H_9 + NO \longrightarrow C_4H_9NO$$

Based on the yield of CH_3OH, the extent of reaction during the constant photolysis time of 5 min was 14%.

When the isobutane was replaced by 1 atm of O_2, methyl nitrate and formaldehyde were detected on the gas chromatograph, but only the former was measured quantitatively. The quantum yield for CH_3ONO_2 formation was determined at a series of temperatures in the range 26 - 150 °C and using a fixed extent of reaction of 14%. The results are shown in Table 2 which gives mean values of three experiments at each temperature. Although the data show considerable variation, there is a slight tendency for $\Phi(CH_3ONO_2)$ to decrease with increasing temperature.

3.4. Kinetic analysis of results

The primary objective of this study was the determination of the rate constant for the reaction of CH_3O with O_2. If photodissociation of CH_3ONO is the only source of methoxy radicals, the kinetic behaviour of CH_3O in

TABLE 2

Quantum yields for CH_3ONO_2 formation in the photolysis of CH_3ONO–O_2 mixtures[a]

Temperature (K)	$\Phi(CH_3ONO_2)$
299	0.29
306	0.33
335	0.32
354	0.28
373	0.29
373	0.30[b]
387	0.25
408	0.26
423	0.22

[a] $[CH_3ONO]_0 = 6 \times 10^{16}$ molecules cm^{-3}; $[O_2]$ = 1 atm.
[b] The initial NO_2 concentration was 3.04×10^{15} molecules cm^{-3}.

CH_3ONO photolysis will be governed to a first approximation by the following reactions:

$$CH_3ONO + h\nu \longrightarrow CH_3O + NO \quad (1)$$

$$CH_3O + O_2 \longrightarrow HCHO + HO_2 \quad (4)$$

$$CH_3O + NO_2 \longrightarrow CH_3ONO_2 \quad (5)$$

$$CH_3O + NO \xrightarrow{(M)} CH_3ONO \quad (6)$$

$$\longrightarrow HCHO + HNO \quad (7)$$

$$HO_2 + NO \longrightarrow NO_2 + OH \quad (8)$$

Steady state analysis yields the following expression for the inverse quantum yield Φ^{-1} for CH_3ONO_2 formation:

$$\Phi^{-1} = 1 + \frac{(k_6 + k_7)[NO]}{k_5[NO_2]} + \frac{k_4[O_2]}{k_5[NO_2]} \quad (I)$$

For the photolysis of low concentrations of CH_3ONO in the presence of O_2 it was found that, over most of the reaction time, $[NO_2] \gg [NO]$. Since $k_6 = (2.03 \pm 0.47)2k_5$ [19] and $k_7 = 0.17\,k_6$ [6, 20], the term involving [NO] in eqn. (I) becomes negligible and a plot of $(\Phi^{-1} - 1)[O_2]^{-1}$, determined from the ratio of the instantaneous rates of change of concentration of CH_3ONO_2 and CH_3ONO, *versus* $[NO_2]^{-1}$ at time t should be linear and should pass through the origin. A plot of selected data from the low concentration experiments is shown in Fig. 3. The expected $[O_2]/[NO_2]$ dependence can be seen and a linear least-squares analysis gave a slope of $(1.04 \pm 0.16) \times 10^{-4}$ and an intercept of $-(0.3 \pm 0.9) \times 10^{-5}$. The ratio k_4/k_5 is well defined by this plot. Although the negative intercept is not significantly different from zero, the possibility of a systematic error rising from this simplified analysis cannot be ruled out.

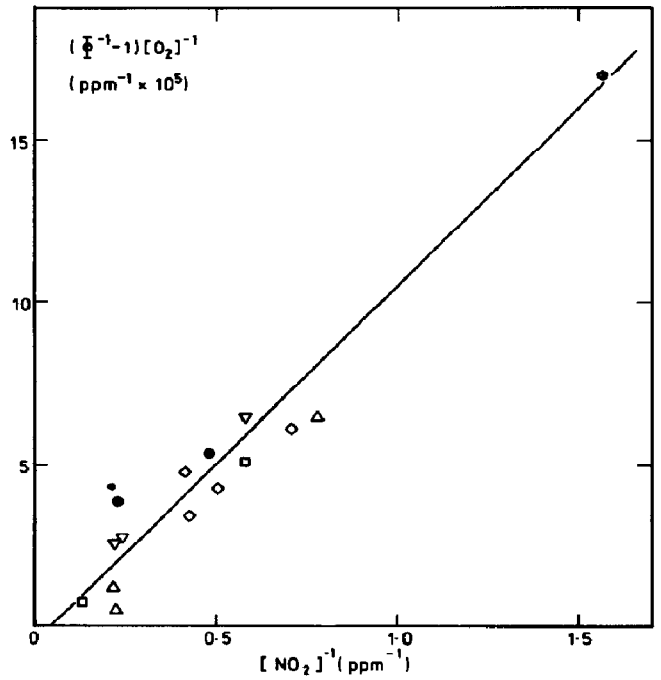

Fig. 3. A plot of $(\Phi^{-1} - 1)[O_2]^{-1}$, where Φ is the quantum yield of methyl nitrate formation during the photolysis of CH_3ONO, *vs.* the inverse of the concentration of NO_2 present. Mole fraction of O_2 in diluent: ○, 0.036; □, 0.10; ▼, 0.20; ▽, 0.25; △, 0.75; ◇, ●, 1.0. Filled points: additional NO_2 present initially.

In the experiments at high concentrations of CH_3ONO, the NO and NO_2 concentrations were not measured. However, it can be readily shown that, since a significant fraction (approximately 30%) of the CH_3O reacted with NO_2 to form CH_3ONO_2, insufficient HO_2 would be produced in reaction (4) to prevent the net production of an appreciable amount of NO from reaction (1). Thus the term involving NO in eqn. (I) cannot be neglected and the data cannot be analysed in a simple fashion.

In order to make best use of all of the available data, a complete mechanism for the photolysis of methyl nitrite–O_2 mixtures was developed by computer simulation techniques utilizing the Harwell programme FACSIMILE [21]. The mechanism was tested against the observed concentration–time behaviour and the rate constants were optimized using the criterion of minimum least-squares deviation between the experimental and computed curves.

3.5. Mechanism for the photolysis of methyl nitrite

In addition to reactions (1) and (4) - (8) the following reactions were incorporated into the kinetic analysis:

$$HO_2 + NO_2 \rightleftharpoons HO_2NO_2 \qquad (9), (-9)$$

$$OH + NO_2 \xrightarrow{(M)} HNO_3 \qquad (10)$$

$$OH + NO \longrightarrow HNO_2 \quad (11)$$

$$OH + HCHO \longrightarrow H_2O + CHO \quad (12)$$

$$\longrightarrow H + HCOOH \quad (13)$$

$$OH + CH_3ONO \longrightarrow H_2O + HCHO + NO \quad (14)$$

$$\longrightarrow CH_3O + HONO \quad (15)$$

$$\xrightarrow{O_2} CH_3ONO_2 + HO_2 \quad (16)$$

$$CHO + O_2 \longrightarrow CO + HO_2 \quad (17)$$

$$H + O_2 \xrightarrow{(M)} HO_2 \quad (18)$$

$$CH_3O + HNO \longrightarrow CH_3OH + NO \quad (19)$$

$$HO_2 + HO_2 \longrightarrow H_2O_2 + O_2 \quad (20)$$

$$NO_2 + h\nu \longrightarrow NO + O \quad (21)$$

$$O + O_2 \xrightarrow{(M)} O_3 \quad (22)$$

$$NO + O_3 \longrightarrow NO_2 + O_2 \quad (23)$$

$$NO_2 + O_3 \longrightarrow NO_3 + O_2 \quad (24)$$

$$NO_3 + NO \longrightarrow 2NO_2 \quad (25)$$

$$NO_3 + NO_2 \rightleftharpoons N_2O_5 \quad (26)$$

$$HONO + h\nu \longrightarrow HO + NO \quad (27)$$

$$CH_3O + HO_2 \longrightarrow CH_3OH + O_2 \quad (28)$$

The absolute rate constants for CH_3O were evaluated using the thermochemical kinetic estimate for k_6 of 2.09×10^{-11} cm^3 molecule^{-1} s^{-1} (± a factor of 2) [22], which is based on measurements of the Arrhenius parameters for the thermal decomposition of CH_3ONO, a calculated entropy change ΔS°_5 and the assumption that $E_5 = 0$. The ratios k_6/k_5 and k_6/k_7 were assumed to be temperature independent. Kinetic data for peroxynitric acid formation and decomposition were taken from two recent studies [23, 24]. The overall rate constants for the reactions of OH with HCHO and CH_3ONO were 1.3×10^{-11} and 1.6×10^{-12} cm^3 molecule^{-1} s^{-1} respectively [25, 26] and the relative rates for the different reaction channels were evaluated as described later. McGraw and Johnston's [20] value of 5×10^{-11} cm^3 molecule^{-1} s^{-1} was employed for reaction of CH_3O with HNO, although this reaction was of negligible importance for most of the experimental conditions. The same value was used for the reaction of CH_3O with HO_2. The alternative fate of HNO is believed to be N_2O formation [6]:

$$2HNO \longrightarrow N_2O + H_2O$$

However, the kinetics of this reaction are unclear and it may be a heterogeneous process. The remainder of the rate constants were taken from a recent CODATA evaluation [25].

The mechanism described accounts for all the products of the photolysis of CH_3ONO–O_2 mixtures which have been observed in this study, in the IR study by Gay *et al.* [7] and also in the study of Wiebe *et al.* [6]. The mechanism also gives the correct kinetic dependence of the reactants and products, as can be seen from the concentration–time curves shown in Fig. 1 which were obtained by computer simulation. The experimental data for CH_3ONO, CH_3ONO_2, NO_2, NO and HNO_3 are well fitted in the simulation. The computed formaldehyde concentration is higher than the experimental value by a constant amount of 0.65 ppm (1.6×10^{13} molecules cm^{-3}), suggesting an interference in the analysis. The simulated curve labelled HNO_3 also includes peroxynitric acid which reached a maximum concentration of 1.5×10^{13} molecules cm^{-3} after 40 min photolysis. The total $HNO_3 + HO_2NO_2$ is seen to give an excellent fit to the experimental points obtained from the loss in measurable NO_x during photolysis.

In the simulation illustrated in Fig. 1, the data for CH_3ONO, CH_3ONO_2, NO_2 and NO were used to obtain optimized values for the photolysis rate k_1 and the rate constant k_4 for the $CH_3O + O_2$ reaction. The experimental value for k_1 of 6.2×10^{-4} s^{-1}, obtained from the first order decay plot of CH_3ONO, was used as initial input, together with $k_4 = 1 \times 10^{-15}$ cm^3 $molecule^{-1}$ s^{-1} based on analysis using eqn. (I); the optimized fit was obtained with values of $(5.2 \pm 0.45) \times 10^{-4}$ s^{-1} and $(1.12 \pm 0.16) \times 10^{-15}$ cm^3 $molecule^{-1}$ s^{-1} respectively (the error limits are 95% confidence limits).

The reduction in k_1 results from the removal of CH_3ONO by OH, reactions (14) - (16). Information on the reaction pathway for this process was obtained from the experimental [NO] *versus* time behaviour in the initial stages of the reaction. Initially the simulation was carried out with reaction (14), involving hydrogen atom abstraction, as the sole pathway for the attack of OH on methyl nitrite. The resultant NO profile is indicated by the dotted curve in Fig. 1 and exhibits completely different behaviour from that observed experimentally, in that the net NO production is much too high in the initial stages. When all three routes (14) - (16) were included and the branching ratios were allowed to "float", keeping the total rate constant $k_{14} + k_{15} + k_{16}$ equal to the value given by Campbell and Goodman [26], the NO behaviour illustrated by the full curve was obtained. The optimized branching ratios were $k_{14}:k_{15}:k_{16} = 1.0:(0.80 \pm 0.10):(0.08 \pm 0.06)$. It is suggested on the basis of these kinetic results that the reaction of OH with CH_3ONO occurs, at least in part, via an addition reaction to form a $CH_3ON(OH)O$ species which can decompose to yield CH_3O + HONO or can react with O_2 to give $CH_3ONO_2 + HO_2$.

The two channels for the attack of OH on formaldehyde were included to account for the observations of Gay *et al.* [7] who have found that an excellent carbon balance can be obtained if secondary oxidation of HCHO leads to both CO and HCOOH as products. The simplest and most reasonable pathway to HCOOH is addition of OH to HCHO followed by hydrogen atom elimination, as suggested by Horowitz *et al.* [27]:

$$HO + HCHO \longrightarrow [H_2C(OH)O] \longrightarrow HCOOH + H \quad \Delta H^\circ = -91 \text{ kJ mol}^{-1}$$

The only loss process for HCHO other than OH attack is direct photolysis, which can be estimated to be relatively slow in these systems on the basis of the known light intensity function and the HCHO absorption cross section. An optimization run on the data of Gay *et al.* [7] to obtain the branching ratio for reactions (12) and (13) gave an excellent fit to their concentration–time curves for HCHO, CO and HCOOH using $k_{13}/k_{12} = 0.20 \pm 0.03$. Thus approximately 18% of the reaction of OH with HCHO at room temperature and atmospheric pressure may occur by addition.

Since the mechanism proposed seems to give a satisfactory explanation of the experimental observations in the CH_3ONO photolysis, it may be employed with some confidence in the optimization procedure for abstracting values of k_4 from all of the CH_3ONO_2 data. It should be emphasized that the absolute value of k_4 is obtained relative to the rate constant k_5 for the addition of CH_3O to NO_2 and that the accuracy is limited to a factor of ±2, arising from the uncertainty in k_5. Tables 3 and 4 show values of k_4 obtained by optimization of the fit to the kinetic data at room temperature (298 ± 3 K) using the low concentration data and at higher temperatures from the high concentration and fixed reaction time data.

At 298 K the value of k_4 shows little or no systematic variation over a 75-fold change in the mean ratio $[NO_2]/[O_2]$ and over a 50-fold variation in the initial CH_3ONO concentration. Also, addition of NO_2 at the start of photolysis does not influence the results. Thus CH_3O seems to be well defined

TABLE 3

Rate constants for the reaction $CH_3O + O_2 \rightarrow HCHO + HO_2$ from computer simulations[a]

$[CH_3ONO] \times 10^{-13}$ (molecules cm^{-3})	$[O_2] \times 10^{-19}$ (molecules cm^{-3})	$[NO_2] \times 10^{-13}$ (molecules cm^{-3})	$[NO_2]/[O_2]$[b] (mean × 10^5)	k_4 (cm^3 $molecule^{-1}$ s^{-1})[c]
19.6	2.5	–	0.16	0.87
22.1	2.5	2.5	0.25	1.03
26.9	2.5	2.5	0.29	1.24
34.6	2.5	2.1	0.35	1.10
42.8	2.5	–	0.39	1.34
20.6	2.5	10.8	0.50	1.34
51.3	1.8	–	0.53	1.41
21.5	0.61	–	0.98	1.20
23.8	0.49	2.2	1.35	1.34
45.3	0.25	–	2.90	1.90
29.6	0.25	3.8	3.0	1.10
12.4	0.09	1.6	3.9	1.71
600	2.4	–	12.0	1.64[d]
			mean =	1.32

[a] Initial conditions at 298 K.
[b] Approximate mean ratio of $[NO_2]/[O_2]$ during the reaction.
[c] Calculated relative to a value of 1.05×10^{-11} cm^3 $molecule^{-1}$ s^{-1} for k_5.
[d] A "high concentration" result.

TABLE 4

Rate constants for the reaction $CH_3O + O_2 \rightarrow HCHO + HO_2$ from computer simulations[a]

Temperature (K)	k_4 (cm^3 $molecule^{-1}$ s^{-1})
306	2.28
335	2.67
354	2.50
373	2.81
373	2.30
387	3.50
408	3.65
423	2.12

[a]Temperature dependence; $[CH_3ONO] = 6 \times 10^{15}$ molecules cm^{-3}; $[O_2] = 1$ atm.

by the competition between reactions with O_2, NO and NO_2 over a wide range of reaction conditions. The mean value for k_4 of 1.32×10^{-15} corresponds to a ratio k_4/k_5 of 1.25×10^{-4} for which we estimate an overall uncertainty of ±30%.

At the higher temperatures the values of k_4 are much less well defined from the computer analysis, since there were insufficient data points at each temperature to define the competition between reactions (4) and (5) in the absence of measurements of $[NO_2]$ during the reaction. Nevertheless, the median values show a slight increase in k_4 with temperature.

Figure 4 shows an Arrhenius plot of all the reported values found for k_4 in the temperature range 298 - 422 K. The present data at 298 K are in excellent agreement with the results of the CH_3ONO photolysis study of Wiebe *et al.* [6] which gives $k_4 = 1.16 \times 10^{-15}$ cm^3 $molecule^{-1}$ s^{-1}, based on their measured values for $k_4/(k_6 + k_7)$ of 4.7×10^{-5} and for $k_7/(k_6 + k_7)$ of 0.145 and the absolute value of k_6 obtained from thermochemical kinetic data from CH_3ONO pyrolysis [22]. The value reported by Kirsch and Parkes [11] is somewhat higher but, considering that effectively it was measured using the reaction of CH_3O with isobutane as a reference for which $k = 3.2 \times 10^{-13}$ $\exp(-2060/T)$ cm^3 $molecule^{-1}$ s^{-1} [28], the agreement can be considered to be satisfactory. Similarly, at 428 K the Kirsch and Parkes [11] value for k_4 of 5.8×10^{-15} cm^3 $molecule^{-1}$ s^{-1} is a little higher than most of the data in this temperature region which were obtained from studies involving CH_3OOCH_3 decomposition [4, 5]. These latter values are based on the thermochemical kinetic estimate of k_6 [22], which was assumed to be independent of temperature. Although somewhat scattered they are in moderately good agreement with each other and with the data obtained at higher temperature in the present work. The k_4 values from the work of Alcock and Mile [10] (at 373 K) and Selby and Waddington [12] (at 410 K), using complex low temperature hydrocarbon oxidation systems, are also consistent with the other data. These data are also relative to hydrogen abstraction by CH_3O from isobutane.

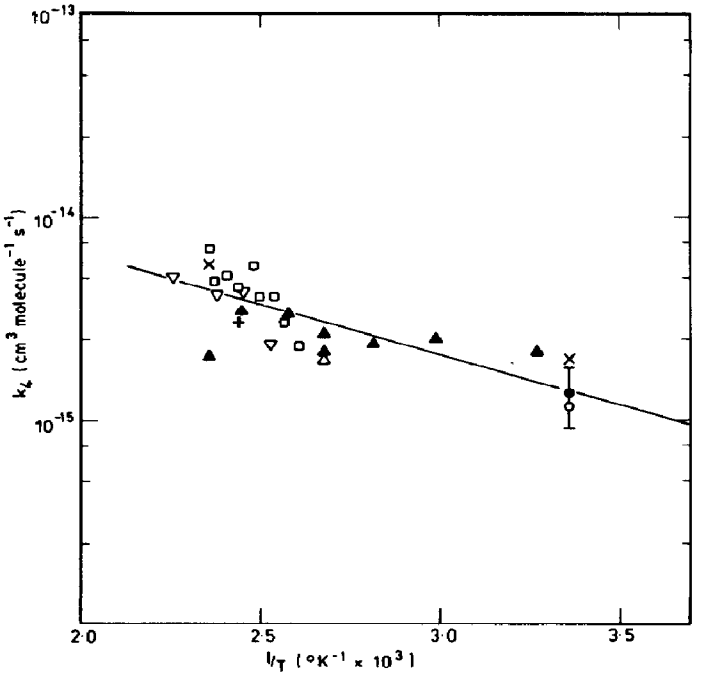

Fig. 4. An Arrhenius plot of data for k_4: •, ▲, this work; □, from ref. 5; ▽, from ref. 6; ×, from ref. 11; +, from ref. 12; ○, from ref. 6; △, from ref. 10.

Least-squares analysis of all of the data with a tenfold weighting factor given to the mean 298 K value from this study gave

$$k_4 = (1.26^{+1.90}_{-0.76}) \times 10^{-13} \exp\{-(1352 \pm 340)/T\}\text{cm}^3 \text{ molecule}^{-1} \text{ s}^{-1}$$

The error limits given are the 2σ confidence limits from the regression analysis. Reaction (4) can occur either by a hydrogen abstraction reaction or via a "trioxide" complex. The transition states involved are

$$CH_3O^{\cdot} + O_2 \longrightarrow [OCH_2\text{---}H\text{---}O_2]^{\dagger} \longrightarrow CH_2O + HO_2$$

$$CH_3O + O_2 \underset{4b}{\overset{4a}{\rightleftharpoons}} CH_3O_3 \xrightarrow{4c} \left[\begin{array}{c} H \\ \diagdown \\ CH_2 \quad O \\ \diagup \quad | \\ O \end{array}\right] \longrightarrow CH_2O + HO_2$$

$$\text{or} \quad \left[\begin{array}{c} H\cdots O \\ \diagdown \\ CH_2 \quad O \\ \diagup \quad | \\ O \end{array}\right] \longrightarrow CH_2\text{—}O\text{—}OOH$$

The Arrhenius factor A for the formation of the cyclic transition state is obtained from $A_{4a}A_{4c}/A_{4b} \approx 10^{-11}\ 10^{12}/10^{14.6} = 10^{-13.6}$. This low A factor rules out the cyclic mechanism. Also, because of the strain energy involved in

ring formation and the activation energy required for the internal hydrogen atom abstraction, the overall activation energy could be high. The results suggest therefore that the reaction of CH_3O with O_2 occurs via simple metathesis.

Acknowledgments

This work was supported by the UK Department of the Environment and by an SRC CASE Studentship to K. G. Patrick.

References

1 J. G. Calvert and J. N. Pitts, *Photochemistry*, Wiley, New York, 1966.
2 R. A. Cox, R. G. Derwent, P. M. Holt and J. A. Kerr, *J. Chem. Soc., Faraday Trans. I, 72* (1976) 2044.
3 J. J. McGarvey and W. D. McGrath, *Trans. Faraday Soc., 60* (1964) 2196.
4 J. R. Barker, S. W. Benson and D. N. Golden, *Int. J. Chem. Kinet., 9* (1977) 31.
5 L. Batt and G. N. Robinson, *Int. J. Chem. Kinet., 11* (1979) 1045.
6 H. A. Wiebe, A. Villa, T. M. Hellman and J. Heicklen, *J. Am. Chem. Soc., 95* (1973) 7.
7 B. W. Gay, R. C. Noonan, P. L. Hanst and J. J. Bufalini, Photolysis of alkyl nitrites and benzyl nitrite at low concentrations: an infrared study, Paper 12, *ACS Symp. Ser. 17* (1975) 132.
8 R. Shortridge and J. Heicklen, *Can. J. Chem., 51* (1973) 2251.
9 J. Weaver, R. Shortridge, J. Meagher and J. Heicklen, *J. Photochem., 4* (1975) 109.
10 W. G. Alcock and B. Mile, *Combust. Flame, 24* (1975) 125.
11 L. J. Kirsch and D. A. Parkes, presented at the *5th Int. Symp. on Gas Kinetics, Manchester, Gt. Britain, 1977.*
12 K. Selby and D. J. Waddington, Reactions of oxygenated radicals in the gas phase, Part 4, *J. Chem. Soc., Perkin Trans. II*, in the press.
13 W. R. Stockwell and J. G. Calvert, *J. Photochem., 8* (1978) 193.
14 H. S. Johnston and R. A. Graham, *Can. J. Chem., 52* (1974) 1415.
15 R. A. Cox, R. G. Derwent and P. M. Holt, *J. Chem. Soc., Faraday Trans. I, 72* (1976) 2031.
16 C. H. Wu and H. Niki, *Environ. Sci. Technol., 9* (1975) 46.
17 R. A. Cox and R. G. Derwent, *J. Photochem., 6* (1976/77) 23.
18 I. T. N. Jones and K. D. Bayes, *J. Chem. Phys., 59* (1973) 4836.
19 L. Batt and G. N. Rattray, *Int. J. Chem. Kinet., 11*, (1979).
20 G. E. McGraw and H. S. Johnston, *Int. J. Chem. Kinet., 1* (1969) 89.
21 E. M. Chance, A. R. Curtis, I. P. Jones and C. R. Kirby, *AERE Rep. R8775*, 1977.
22 L. Batt, R. T. Milne and R. D. McCulloch, *Int. J. Chem. Kinet., 9* (1977) 567.
23 R. A. Graham, A. M. Winer and J. N. Pitts, Jr., *J. Chem. Phys., 68* (1978) 4505.
24 R. A. Cox and K. Patrick, *Int. J. Chem. Kinet., 11* (1979) 635.
25 *CODATA Bulletin no. 33: Evaluated Kinetic Data for Atmospheric Chemistry*, International Council of Scientific Unions, Paris, 1979.
26 I. M. Campbell and K. Goodman, *Chem. Phys. Lett., 36* (1975) 382.
27 A. Horowitz, Fu Su and J. G. Calvert, *Int. J. Chem. Kinet., 10* (1978) 1099.
28 T. Berces and A. F. Trotman-Dickenson, *J. Chem. Soc.*, (1961) 348.